Journal of Material Science and Mechanical Engineering (JMSME)
p-ISSN: 2393-9095; e-ISSN: 2393-9109; Volume 10, Issue 1; January-March, 2023, pp. 17-21

http://www.krishisanskriti.org/Publication.html

Effect of Welding Speed on Corrosion Behaviour of Friction Stir Welded Joints of Dissimilar Aluminium Alloys

Qamar Alam[1], Ketan Sherma[1], Afreen Ikram[1], Tanveer Majeed[1*], Yashwant Mehta[1]

[1]Department of Metallurgical and Materials Engineering, National Institute of Technology, Hazratbal, Srinagar, 190006, Jammu and Kashmir, India
E-mail: tanveer_02phd18@nitsri.net

Abstract—*The present study analyzes the effect of welding speed on the corrosion behaviour of dissimilar joints of aluminium (Al) alloys welded via friction stir welding (FSW). FSW was performed between AA2024-T3 and AA7475-T7 alloy plates at different welding speed i.e., 50, 63 and 80 mm/min. The influence of welding speed on corrosion behaviour of FSWed joints was examined by performing potentiodynamic polarization test, microstructural characterizations, field emission scanning electron microscopy (FESEM) and energy-dispersive spectroscopy (EDS). The surface features and microstructural examination of the specimens revealed pitting corrosion in the base materials as well stir zones of welded specimens. It was further observed form potentiodynamic polarization test that the corrosion rate of joints increases with the welding speed.*
Keywords: *Aluminium alloys, friction stir welding, welding speed, corrosion behaviour microstructure*

1. Introduction

The desirable properties of aluminium (Al) alloys such as lightweight, low weight to strength ratio and acceptable corrosion resistance have resulted in considerable reductions in fuel consumption, energy usage, and weight in transportation industry [1]. In recent years Al alloys have largely replaced traditional materials such as steels in the aviation and transportation industries. However, conventional fusion welding techniques are no longer appropriate to weld Al alloys involving formation of various defects such as porosity, solidification cracking and softening effect [2]. To meet the demand of lightweight body structures for aviation and automotive sectors, friction stir welding (FSW) emerged as potential technique to join high strength Al alloys in different joint configurations. FSW is a novel solid state welding process that was developed and by the welding institute (TWI) in 1991. Based on microstructural features, the FSWed joint consist of four different weld regions i.e., the nugget zone (NZ), the thermo-mechanically affected zone (TMAZ), the heat affected zone (HAZ), and the base material (BM). The central NZ consists of refined and dynamically recrystallized grains owing to high induced heat input and intense plastic deformation in this zone. The TMAZ surrounding the SZ comprises of elongated and diffused grains which is attributed to low heat input and partial plastic deformation. The HAZ consists of large grains subjected to thermal cycles without plastic deformation.

Although, the various benefits of FSW, the joints are susceptible to corrosion owing to intense plastic deformation and complex material flow. In the case of FSW of heat treatable Al alloys, the corrosion susceptibility of joints is attributed to heterogeneous distribution of second phase particles resulting heterogeneity in microstructure leading to increased susceptibility of joints to local corrosion attack such as pitting, intergranular corrosion (IGC), etc [3]. In FSW, process parameters i.e., rotational speed, tool shoulder diameter, welding speed, plunge depth, tool tilt angle, etc have significant effect on heat input, intense plastic deformation and distribution of second phase particles (SPPs). For instance, [4] studied the effect of welding parameters on average size of SSPs in NZ of weld (AA2014) and it was demonstrated that the size of SPPs increases with tool rotational speed. [5] studied the effect of welding speed on corrosion behaviour of AA2219-O joints and it was reported that corrosion resistance of joints decreased with the increase in welding speed. Recently, Majeed et al., (2022) [6] studied the effect of shoulder diameter on electrochemical behaviour of unequal thickness dissimilar joints. The Authors reported that corrosion resistance decreased with the increase in tool shoulder diameter which is attributed to increase in grain size with shoulder diameter. From above literature review, effect of welding parameters on electrochemical behaviour of FSWed joints has been investigated yet no research has been done to date revealing the effect of welding speed on electrochemical behaviour of dissimilar joints of AA2024-T3 and AA7475-T7 alloys. In the present study, effect of welding speed on the corrosion behaviour of dissimilar joints of AA2024-T3 and AA7475-T7 using FSW was investigated in detail by exposing the NZs of welded joint to 3.5 M NaCl electrolyte solution for three hours. In addition, the

electrochemical behaviour of FSWed joints was revealed via potentiodynamic polarization test, microstructural analysis, field emission scanning electron microscopy (FESEM), and energy-dispersive spectroscopy (EDS).

2. Experimental Work

2.1 Materials and Equipment

Dissimilar Al alloys plates of AA2024-T3 and AA7475-T7 alloys having dimensions of 180 x 50 x 2.5 mm were joined using Friction Stir Welding on conventional vertical milling machine retrofitted with tool adopter. The elemental composition of the base materials (BMs) is illustrated in Table 1. The FSW of dissimilar Al alloys was carried out using a non consumable tool made of high speed steel having well defined shoulder and pin profile (taper cylindrical). Details of the process parameters are presented in Table 2. In this study, effect of welding speed on corrosion behaviour of FSWed joints was assessed by conducting FSW at three different levels of welding speeds i.e., 50, 63 and 80 mm/min (refer to Table 2).

Table 1: Elemental composition of BMs (Wt %)

Alloy	Cu	Mn	Si	Cr	Zn	Ni	Fe	Mg	Zr	Ti	Al
AA2024-T3	4.57	0.51	0.074	0.005	0.002	0.014	0.204	1.10	-	0.04	Bal.
AA7475-T7	1.34	0.0062	0.06	0.155	5.36	0.002	0.101	1.93	0.0076	0.023	Bal.

Table 2: FSW process parameters

Specimen	Welding speed (mm/min)	Rotational speed (rpm)	Tool tilt angle (α)	Shoulder Diameter (mm)
S-1	50	710	3º	18
S-2	63	-	-	-
S-3	80	-	-	-

2.2 Preparation of the Surface Specimen

After FSW, the specimens were sectioned from transverse cross section of the weld plates using wire electric discharge machine. The specimens were prepared by following standard metallographic procedures. The specimens were initially grinded with emery papers having grit sizes: 320, 400, 600, 800, 1000, 1200 and 1500 followed by cloth polishing using 1.0 µm alumina powder. Finally, the specimens were polished with 0.25 µm diamond paste on velvet cloth. Thereafter, specimens were chemically etched using Keller's solution for revealing the surface morphologies of joints using optimal microscopy, FESEM and EDS.

2.3 Corrosion Analysis

For the purpose of electrochemical measurements, a three electrode electrochemical cell was employed, incorporating platinum electrodes as counter electrode, saturated calomel electrode (SCE) as standard reference electrode and specimens as working electrode as shown in Fig. 1. The specimens were separately exposed to 3.5 M NaCl electrolyte solution for 3.5 hours maintained at 25°C. Potentiodynamic curves were obtained post immersion at the scan rate of 0.3 mV/s. The potentiostatic test was employed to scan the potential of working electrode from -250 mV to 250 mV.

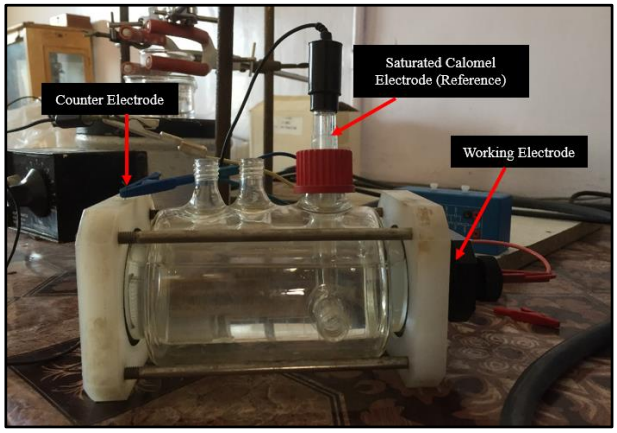

Figure 1: Depicts the experimental setup for the corrosion test

3. Results and discussion

3.1 Metallographic Investigation

The microstructures of BMs and NZs of the FSWed specimens were examined using optical microscope. The microstructural images of the specimens before and after exposing to 3.5 M NaCl solution for 3.5 hours are depicted in the Fig.2 and Fig.3, respectively. NZs of FSWed joints consist of fine and equiaxed grain owing to high heat input and intense plastic deformation during FSW. The surface morphology of specimens reveals that BM AA7475-T7 was severely corroded (pitting) in contrast to BM AA2024-T3. NZ of S-3 specimens produced at welding speed of 80 mm/min was most severely corroded (pitting) followed by S-2 and S-1 specimens as illustrated in Fig. 3.

The average grain size of NZs of welded specimens was measured using ImageJ software to explore the effect of welding speed on electrochemical behaviour of joints. Table 3 presents the average grain size of NZs of S-1, S-2 and S-3 specimens demonstrating that average grain size increases with increase in welding speed. The smallest average grain size was obtained at 50 mm/min which is attributed to combined effect of adequate heat input and plastic deformation of material during FSW [7]. Further increase in welding speed leads to decrease in heat input and material

deformation rate. The reduction in material deformation rate with increase in welding speed favours the grain as per the recrystallization principle [8]. This increase in grain size with welding speed reduces corrosion resistance as was demonstrated by Kish et al., (2014) [9]. It has been observed that fine grain favours the growth of passive protective layer owing to high density grain boundary in NZ resulting in high corrosion resistance.

Table 3. Illustrate the average grain size of NZs of weld specimens

Specimens	Welding Speed(mm/min)	Grain size(μm)
S-1	50	3.57
S-2	63	3.80
S-3	80	4.57

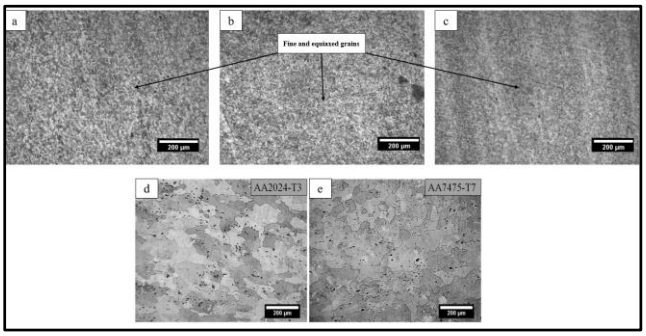

Figure 2: Illustration the microstructures of the NZs of (a) S-1, (b) S-2, (c) S-3 welded specimens (d) BM AA2024-T3 and (e) BM AA7475-T7 potentiodynamic test

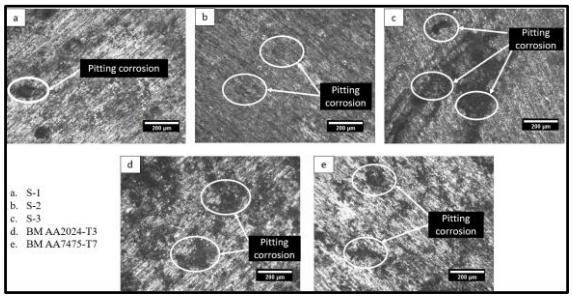

Figure 3: Illustration the microstructures of the NZs of (a) S-1, (b) S-2, (c) S-3 welded specimens (d) BM AA2024-T3 and (e) BM AA7475-T7 after potentiodynamic test

FESEM images as shown in Fig.4 reveals pitting corrosion on the surface of the NZs of the weld specimens and the BMs. Pitting corrosion in NZs of FSWed joints is attributed to galvanic coupling between precipitates and Al matrix resulting in dissolution of BM matrix [4]. Further, it is evident from Fig. 4 that the severity of the pitting increases as the welding speed increases, i.e., S-3 specimen shows the highest intensity of the pits followed by S-2 and S-1 specimens. This behaviour is attributed to the fact that as the welding speed increases the mechanical stirring forces decreases resulting in formation of large precipitates and higher pitting corrosion as was claimed by Weifeng et al, (2010) [5]. Moreover, the presence of large precipitates hampers the formation of continuous passive protective layers leading to increased susceptibility to corrosion [10]. In addition, BM-AA7475-T7 shows higher pit intensity than BM-AA2024-T3. Corrosion susceptibility of the BMs is attributed to the large potential difference between the metal matrix and precipitates give rise to galvanic couple where the more negative Cu-rich phases like θ(Al_2Cu), S(Al_2CuMg) and $MgZn_2$ phases undergo dissolution with respect to less negative metal matrix [3].

From the EDS analysis, as depicted in Fig. 5, it is quite clear that as the welding speed increase the wt % of Cu and Zn decreases indicating an increase in dissolution rate of Cu and Zn rich precipitates with welding speed. This can be explained by the fact that large Cu rich precipitates obtained at higher welding speed undergo severe pitting as was reported by Svenningsen et al., (2006)[11]. Further, the increase in size of precipitates with welding speed favours the galvanic effect where more negative anodic dissolution of Al matrix leads to severe pitting.

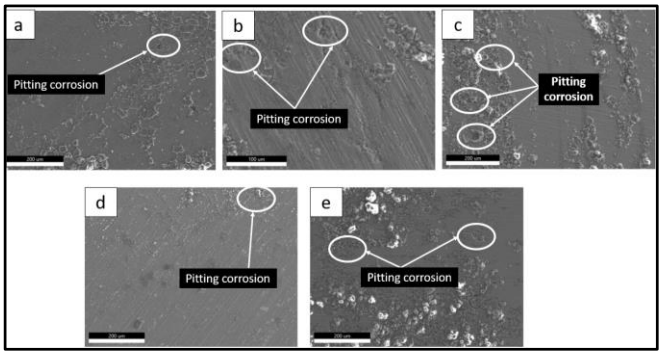

Figure 4: SEM images obtained for the SZs of (a) S-1 (b) S-2 (c) S-3 of welded surfaces (d) BM-AA2024-T3 (e) BM AA7475-T7

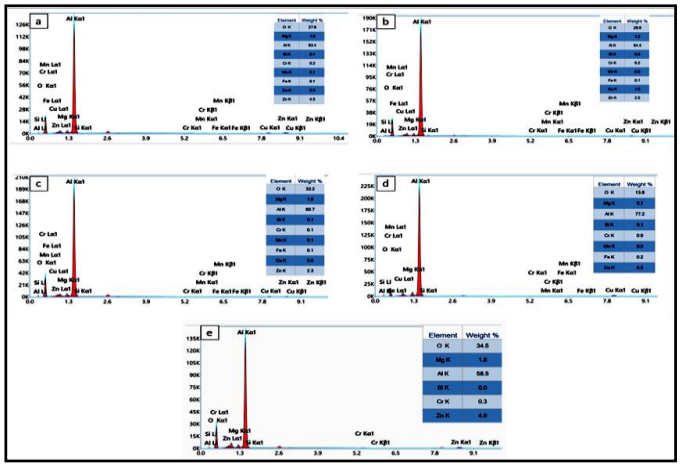

Figure.5 : Show EDS data for (a) S-1 (b) S-2 (c) S-3 (d) BM AA2024-T3 (e) BM AA7475-T7

3.2 Electrochemical Analysis

Potentiodynamic tests were performed by exposing the NZs of the weld specimens and the BMs to 3.5 M NaCl electrolyte solution for 3.5 hours. Fig.6 shows the potentiodynamic polarization curves obtained using Tafel extrapolation method. Table 4 gives $i_{corr,}$ E_{corr} and corrosion rate (mmy) values obtained from the potentiodynamic curves using Tafel extrapolation techniques using EC Lab software. From the Table 4, it is quite evident that the BM-AA7475-T7 has higher i_{corr} value indicating lesser corrosion resistance than BM-AA2024-T3 that has lower value of i_{corr} [12]. Further, it is evident that among the weld specimens the specimen S-3 has the highest $i_{corr,}$ indicating the least corrosion resistance followed by S-2 and S-1 specimen. This demonstrates that increasing welding speed 50 to 80 mm/min leads to increase in corrosion rate, due to the fact that at low welding speed, the high induced heat leads to dissolution of precipitates resulting in high corrosion resistance of joint as was reported by Patil and Soman et al., (2013)[13].

Table 4. E_{corr}, i_{corr}, and corrosion rate of specimens after being exposed to 3.5 M NaCl electrolyte

Specimens	S1	S2	S3	BM AA2024 T3	BM AA7475 T7
I_{corr} ($\mu A/cm^2$)	1.866	2.671	3.106	2.221	3.237
E_{corr} (mV)	-751.154	-787.152	-825.182	-624.047	-755.015
Corrosion rate (mpy)	0.81711	1.16961	1.36009	0.96611	1.42199

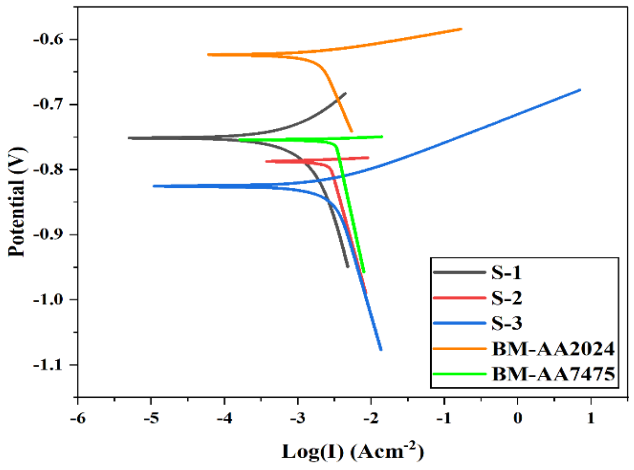

Figure 6: Potentiodynamic polarization curves of BMs and weld specimens

4. Conclusion

The effect of welding speed on electrochemical behaviours of NZs and BMs were characterized via potentiodynamic polarization test, microstructural, FESEM and EDS analysis of the weld specimens and the BMs and the following conclusions were drawn:

1. The microstructural characterization shows severe pitting corrosion in all the specimens. Moreover, NZ of S-3 shows more severe pitting followed by S-2 and S-1 specimens. Further, average grain size was observed to increase with increase in welding speed.
2. The FESEM analysis of welded specimens reveals increase in corrosion susceptibility of NZs with welding speed. EDS analysis confirms the increased dissolution of Cu and Zn rich precipitates with welding speed.
3. The potentiodynamic polarization results of the weld specimens showed that corrosion rate increase with welding speed. In addition, the corrosion rate of BM AA7475-T7 was more as compared to BM AA2024-T3.

References

[1] R.S. Mishra, Z.Y. Ma, Friction stir welding and processing, Mater. Sci. Eng., R 50(1-2) (2005) 1–78.

[2] S. Bag, E.T. Akinlabi, Eco-friendly aspects in hybridization of friction stir welding technology for dissimilar metallic materials, Encycl. Renewable Sustainable Mate. 1 (2020) 225–236, https://doi.org/10.1016/B978-0-12- 803581-8.11153-1.

[3] Tanveer Majeed, Yashwant Mehta, Arshad Noor Siddiquee. Precipitation-dependent corrosion analysis of heat treatable aluminum alloys via friction stir welding, a review, Proc IMechE Part C: J Mechanical Engineering Science 0(0) 1–27. DOI: 10.1177/09544062211003609

[4] Sinhmar S and Dwivedi DK. Effect of weld thermal cycle on metallurgical and corrosion behavior of friction stir weld joint of AA2014 aluminium alloy. J Manuf Process 2019; 37: 305–320.

[5] Xu W, Liu J and Zhu H. Pitting corrosion of friction stir welded aluminum alloy thick plate in alkaline chloride solution. Electrochim Acta 2010; 55: 2918–2923.

[6] Tanveer Majeed, Yashwant Mehta, Arshad Noor Siddiquee. Electrochemical Behaviour of Friction Stir Welded Joints: Effect of Tool Shoulder Diameter Materials Today Proceedings, 62 (2022) 26-31.

[7] Yingli Li , Hongge Yan, Jihua Chen, Weijun Xia, Bin Su, Tian Ding and Xinyu Li. Influences of welding speed on microstructure and mechanical properties of friction stir welded Al–Mg alloy with high Mg content. Mater. Res. Express 7 (2020) 076506. https://doi.org/10.1088/2053-1591/ab9854

[8] Heidarzadeh A, Testik Ö M, Güleryüz G and Barenji R V 2020 Development of a fuzzy logic based model to elucidate the effect of FSW parameters on the ultimate tensile strength and elongation of pure copper jointsJ. Manuf. Process. 53 250–9

[9] Kish JR, Williams G, McDermid JR, Thuss JM, Glover CF, Williams G, Effect of grain size on the corrosion resistance of friction stir welded Mg alloy AZ31B joints. Journal of Electrochemical Society, 2014,161: 405–411.

[10] Wloka, J., Virtanen, S., 2007, Influence of scandium on the pitting behaviour of Al-Zn-Mg-Cu alloys. Acta Materiallia, Vol. 55, 6666-6672.

[11] Gaute Svenningsen, John Erik Lein, Astrid Bjørgum, Jan Halvor Nordlien, Yingda Yu, Kemal Nisancioglu. Effect of low copper content and heat treatment on intergranular corrosion of model AlMgSi alloys. Corros Sci 2006; 48: 226–242.

[12] H. Fang, B. Brown and S. Nesic. Sodium Chloride Concentration Effects on General CO2 Corrosion Mechanisms. Corrosion 69, 297-302

[13] Patil HS and Soman SN. Effect of weld parameter on mechanical and metallurgical properties of dissimilar joints AA6082–AA6061 in T6 condition produced by FSW. *Frattura ed Integrita Strutturale* 2013